HHS Public Access

Author manuscript

Oncogene. Author manuscript; available in PMC 2016 May 05.

Published in final edited form as:

Oncogene. 2015 November 5; 34(45): 5617–5625. doi:10.1038/onc.2015.32.

HSPB1 as a Novel Regulator of Ferroptotic Cancer Cell Death

Xiaofang Sun[1,*], **Zhanhui Ou**[1], **Min Xie**[2], **Rui Kang**[4], **Yong Fan**[1], **Xiaohua Niu**[1], **Haichao Wang**[3], **Lizhi Cao**[2], and **Daolin Tang**[1,4,*]

[1]Key Laboratory for Major Obstetric Diseases of Guangdong Province, Key Laboratory of Reproduction and Genetics of Guangdong Higher Education Institutes, The Third Affiliated Hospital of Guangzhou Medical University, Guangzhou, Guangdong 510510, China

[2]Department of Pediatrics, Xiangya Hospital, Central South University, Changsha, Hunan 410008, China

[3]Department of Emergency Medicine, North Shore University Hospital, and The Feinstein Institute for Medical Research, Manhasset, New York 11030, USA

[4]Department of Surgery, University of Pittsburgh Cancer Institute, University of Pittsburgh, Pittsburgh, Pennsylvania 15213, USA

Abstract

Ferroptosis is an iron-dependent form of non-apoptotic cell death, but its molecular mechanism remains largely unknown. Here, we demonstrate that heat shock protein beta-1 (HSPB1) is a negative regulator of ferroptotic cancer cell death. Erastin, a specific ferroptosis-inducing compound, stimulates heat shock factor 1 (HSF1)-dependent HSPB1 expression in cancer cells. Knockdown of HSF1 and HSPB1 enhances erastin-induced ferroptosis, whereas heat shock pretreatment and overexpression of HSPB1 inhibits erastin-induced ferroptosis. Protein kinase C-mediated HSPB1 phosphorylation confers protection against ferroptosis by reducing iron-mediated production of lipid reactive oxygen species. Moreover, inhibition of the HSF1-HSPB1 pathway and HSPB1 phosphorylation increases the anticancer activity of erastin in human xenograft mouse tumor models. Our findings reveal an essential role for HSPB1 in iron metabolism with important effects on ferroptosis-mediated cancer therapy.

Introduction

Cell death occurs in many forms with different hallmarks depending on the type of stress (1, 2). In addition to apoptosis, several types of caspase-independent programmed cell death have recently been identified to regulate various physiological and pathological processes (3–5). Among them is ferroptosis, coined by Scott J. Dixon, Brent R. Stockwell, and colleagues in 2012, which refers to an iron-dependent novel form of non-apoptotic cell death (6). Ferroptosis is significantly distinct at morphological, biochemistral, and genetic levels

Correspondence to: Daolin Tang (tangd2@upmc.edu) or Xiaofang Sun (xiaofangsun@hotmail.com).

Conflict of Interest: The authors declare no conflicts of interest.

from other forms of cell death such as apoptosis and necrosis (6). For example, the classic morphological and biochemical features of apoptosis (e.g., chromatin fragmentation, mitochondrial cytochrome c release, caspase activation, and poly ADP ribose polymerase cleavagation) and necrosis (e.g., disruption of the cellular membrane, swelling of the cytoplasm and mitochondria, cellular energy depletion) are not observed in ferroptosis (6). This process is characterized by the overwhelming, iron-dependent accumulation of lethal lipid reactive oxygen species (ROS) (6). Erastin functions as a specific ferroptosis activator by acting on mitochondrial voltage-dependent anion channels or cystine/glutamate antiporters, exhibiting selectivity for several tumor cells bearing oncogenic RAS (7–10). The morphological features of erastin-treated cells include smaller cell size and smaller mitochondria with increased membrane density and loss of structural integrity (6, 9). In contrast, ferrostatin-1 is a potent and selective inhibitor of ferroptosis through preventing erastin-induced accumulation of lipid ROS, but not chelating iron (6). Several genes or proteins responsible for the regulation of iron and lipid ROS metabolism have been implicated in ferroptosis (11). For instance, glutathione peroxidase 4 has been identified as a negative regulator of ferroptosis by limiting lipid ROS production (12), but the intricate regulatory mechanisms of ferroptosis remain largely unknown. Necroptosis is a form of regulated necrosis that can be activated by ligands of death receptors under apoptotic deficient conditions. Recent studies indicate that ferroptosis, but not necroptosis, contributes to acute renal failure and renal tubular cell death after ischemia (13, 14). This result indicates that different types of regulated death may be involved in different tissue ischemia reperfusion injuries.

Heat shock proteins (HSPs) are constitutively expressed under normal conditions, but are inducibly overexpressed under stressful conditions such as heat shock, pH shift, and hypoxia (15). Based on their molecular mass, HSPs are generally divided into six families, namely HSP100, HSP90, HSP70, HSP60, HSP40, and the small heat shock proteins. Heat shock factors (HSFs) are the master transcriptional factors that regulate the inducible synthesis of these HSPs during stress (16). HSPs mainly function as molecular chaperones and protect cells against harmful stimuli by stabilizing unfolded or misfolded peptides and repairing denatured proteins or promoting their degradation (15). Inducible HSPs have been reported to render cancer cells resistant to apoptosis and necrosis in both chaperone activity-dependent and -independent ways (17), but their roles in ferroptosis has not yet been investigated.

In this study, we demonstrate that HSPB1 (also called mouse HSP25 or human HSP27), a member of the small heat shock proteins, is highly inducible following erastin treatment in several types of cancer cells. Phosphorylated HSPB1 acts as a negative regulator of ferroptosis by reducing cellular iron uptake and lipid ROS production. Inhibition of HSPB1 expression and phosphorylation *in vitro* and *in vivo* increases the anticancer activity of erastin-mediated ferroptosis. Our findings present a novel role for HSPB1 in the regulation of ferroptosis with important effects on erastin-mediated anticancer therapy. Our findings also provide new insight into how cancer cells are able to avoid the ferroptotic cell death process.

Results

Erastin induces HSF1-dependent HSPB1 expression in human cancer cells

To determine whether erastin induces HSP expression in cancer cells, human cervical carcinoma HeLa cells were treated with erastin for eight and 24 hours, and the mRNA levels of HSP100 (e.g., ClpB), HSP90, HSP70, HSP60, HSP40, and HSPB1 were analyzed by quantitative real time polymerase chain reaction (Q-PCR). Among these HSPs, HSPB1 was the most highly-induced gene (Fig. 1A). Consistently, Western blot analysis revealed that the protein level of HSPB1, but not HSP90 and HSP70, was significantly increased in HeLa cells following erastin treatment (Fig. 1B). In addition, erastin also induced the expression of HSPB1, but not HSP90 and HSP70, in other human cancer cell lines including U2OS (osteosarcoma) and LNCaP (prostate adenocarcinoma) (Fig. 1B). To determine whether HSF1, the master regulator of heat-induced HSP expression (16), was required for erastin-induced HSPB1 expression, a target-specific shRNA against HSF1 was transfected into HeLa, U2OS and LNCaP cells. The knockdown of HSF1 significantly inhibited erastin-induced HSPB1 mRNA (Fig. 1C) and protein (Fig. 1D) expression. Collectively, these findings suggest that the HSF1-dependent HSPB1 expression may be involved in the regulation of erastin-induced ferroptosis.

Inhibition of HSF1-dependent HSPB1 expression increases erastin-induced ferroptosis

To characterize the role of the HSF1-HSPB1 pathway in ferroptosis, erastin-induced growth inhibition was assayed using an alamarBlue Cell Viability Assay Kit. The downregulation of HSF1 (Fig. 2A) and HSPB1 (Fig. 2B) by specific shRNAs increased erastin-induced growth inhibition in HeLa (Fig. 2C), U2OS (Fig. 2D), and LNCaP cells (Fig. 2E), suggesting that the HSF1-HSPB1 pathway might be a negative regulator of erastin-induced cancer cell death. Indeed, the knockdown of HSF1 and HSPB1 similarly increased erastin-induced intracellular concentrations of iron (Fig. 2F) and lipid ROS (Fig. 2G), two surrogate markers for ferroptosis (6). As expected, the increase in cellular iron in HSPB1 knockdown cells was associated with increased expression of transferrin receptor protein 1 (TFR1) and a mild decrease in the expression of ferritin heavy chain 1 (FTH1) (Fig. 2H). Unlike staurosporine (an inducer for apoptosis) or hydrogen peroxide (H_2O_2, an inducer for necrosis), erastin did not significantly elevate the caspase 3 activity (as a marker for apoptosis, Fig. 2I) and lactate dehydrogenase (LDH) release (as a marker for necrosis, Fig. 2J). LDH is a soluble cytosolic enzyme that is released into the culture medium following loss of membrane integrity resulting from necrosis. Our data of LDH release is consistent with a previous finding that necrosis is not observed in cancer cells following erastin treatment (6). In addition, secondary lipid oxidation products (e.g., 4-hydroxy-2-nonenal) (6) may also inactivate LDH (18).

Moreover, treatment with deferoxamine (an iron-chelating agent) and ferrostain-1 (an inhibitor of ferroptosis), but not Z-VAD-FMK (a general caspase inhibitor), necrostain 1s (Nec-1s, an inhibitor of necroptosis), or cyclosporin A (CsA, an inhibitor of cyclophilin D), prevented erastin-induced growth inhibition in HSF1 and HSPB1 knockdown HeLa (Fig. 2K) and U2OS (Fig. 2L) cells. Thus, these findings indicate that the inhibition of HSF1-

dependent HSPB1 expression specifically increased erastin-induced ferroptosis but not other types of cell death (e.g., apoptosis, necrosis and necroptosis) in cancer cells.

HSPB1 overexpression inhibits erastin-induced ferroptosis

To further characterize the role of HSPB1 in ferroptosis, we first determined whether heat shock-induced HSPB1 expression would inhibit erastin-induced ferroptosis. Heat shock pretreatment at 42.5°C for one hour significantly increased HSF1 phosphorylation at Ser326 (a marker for increased HSF1 transcription activity by heat stress (19)) (Fig. 3A) and mRNA expression of HSPs including HSP70 (Fig. 3B) and HSPB1 (Fig. 3C) at a recovery times of eight to 24 hours. Importantly, heat shock pretreatment reduced erastin-induced growth inhibition (Fig. 3D and 3E), suggesting a protective effect of the heat shock response in the regulation of ferroptosis. In contrast, the knockdown of HSF1 and HSPB1 by shRNA remarkably reversed the heat shock pretreatment-mediated protective effect following erastin treatment (Fig. 3F and 3G). Furthermore, overexpression of HSPB1 by transfection of HSPB1-cDNA inhibited erastin-induced growth inhibition in HeLa cells (Fig. 3H), further confirming HSPB1 as a negative regulator of erastin-induced ferroptosis.

HSPB1 phosphorylation mediates resistance to erastin-induced ferroptosis

In response to erastin, the levels of phosphorylation and expression of HSPB1 were elevated in HeLa cells (Fig. 1 and Fig. 4A). To gain insight into the intricate molecular mechanism by which HSPB1 regulates erastin-induced ferroptosis in cancer cells, we next explored whether alterations in the phosphorylation of HSPB1 influences ferroptosis. Previous studies have indicated that HSPB1phosphorylation during stress is regulated by several kinases such as PKC (20). Consistently, PKC inhibitors (e.g., Gö 6983 and calphostin C) significantly blocked HSPB1 phosphorylation (Fig. 4A) and increased growth inhibition following erastin treatment (Fig. 4B). Furthermore, the expression of phosphorylation-deficient mutants of HSPB1 (S15A/S86A) did not suppress erastin-induced ferroptosis, whereas wild-type HSPB1 cDNA did (Fig. 4C). Phosphorylation of HSPB1 positively modulates actin polymerization and reorganization, which limits iron uptake (21, 22). As expected, the suppression of HSPB1 phosphorylation by PKC inhibitors (e.g., Gö 6983 and calphostin C) and disruptions of actin cytoskeleton by cytochalasin D similarly increased intracellular iron (Fig. 4D), lipid ROS production (Fig. 4E), and growth inhibition (Fig. 4F). Members of the Wiskott-Aldrich syndrome protein (WASP) family activate the Arp2/3-complex leading to actin polymerization (23). To further confirm the role of actin polymerization in ferroptosis, we genetically knocked down WAVE2, a key member of WASP in mammals. Suppression of WAVE2 expression by shRNA (Fig. 4G) in HeLa cells increased intracellular iron (Fig. 4H) and growth inhibition (Fig. 4I) following erastin treatment. These findings suggest that phosphorylation of HSPB1 contributes to ferroptosis resistance through inhibiting cytoskeleton-mediated iron uptake and lipid ROS production.

Suppression of the HSF1-HSPB1 pathway increases anticancer activity of erastin in vivo

To test if suppression of HSF1 and HSPB1 expression also increased tumor sensitivity to erastin *in vivo*, the HSF1 and HSPB1 stable knockdown HeLa cells were implanted into the subcutaneous space of the right flank of mice. Beginning at day seven, these mice were

treated with erastin. Compared with the control shRNA group, erastin treatment effectively reduced the size of tumors formed by HSF1 and HSPB1 knockdown cells (Fig. 5A). Q-PCR analysis of the expression of PTGS2, a marker for assessment of ferroptosis *in vivo* (12), indicated that the knockdown of HSF1 and HSPB1 increases ferroptosis (Fig. 5B). Moreover, KRIBB3, an inhibitor of blocking protein kinase C-dependent phosphorylation of HSPB1 (24), dose-dependently increased erastin-induced tumor inhibition (Fig. 5C), which was associated with an increased PTGS2 mRNA expression (Fig. 5D). Together, these findings demonstrated that the HSF1-HSPB1 pathway is important in modulating the anticancer activity of erastin-mediated ferroptosis *in vivo.*

Discussion

The cellular stress response is a complicated network involved in the activation of survival pathways and the initiation of cell death (25, 26). In this study, we demonstrated that the activation of the HSF1-HSPB1 pathway negatively regulated erastin-induced ferroptosis. In addition, we demonstrated that the PKC-mediated HSPB1 phosphorylation was required for conferring resistance to erastin-induced ferroptosis, possibly through regulating iron-mediated lipid ROS production. In particular, genetic knock-down or pharmacologic inhibition of the HSF1-HSPB1 pathway significantly increased the anticancer activity of erastin *in vitro* and *in vivo*. These data not only reveal a novel role for HSPB1 in ferroptosis, but also suggest the inherent regulatory mechanism of HSPB1 as a potential therapeutic target against cancer.

Ferroptosis was first described in engineered human foreskin fibroblasts as a unique response to oncogenic RAS selective lethal compounds such as erastin (8) as distinguishable from all other types of cell death (6). Subsequently, others (6, 10, 12) have confirmed that erastin also induces ferroptosis in RAS-carrying cancer cells such as HeLa, U2OS, and LNCaP cells. In the present study, we discovered that erastin treatment also induces a significant heat-shock response in cancer cells. As a set of well-ordered and regulated responses to stress, the heat-shock response is characterized by the sequential activation of HSF1 and production of HSPs (15, 16). Our findings suggest that HSF1-dependent HSPB1 expression can also protect tumor cells against erastin-mediated ferroptosis, because the inhibition of the HSF1-HSPB1 pathway significantly enhanced the anticancer activity of erastin *in vitro* and *in vivo*. Given that heat shock pretreatment similarly protects tumor cells against erastin-induced ferroptosis, it will be important to explore the possible role of other HSPs in the regulation of the ferroptotic response.

Until recently, HSPB1 has been considered a molecular chaperone involved in regulation of the organization of the cytoskeleton (27) or stabilizing aberrantly folded proteins to prevent aggregation (28). Upon phosphorylation, however, HSPB1 oligomers dissociate into monomers, which then functions as an inhibitor of apoptosis (29) and inducer of autophagy (30). The phosphorylation of HSPB1 is dynamic and regulated by different kinases such as MAPKAPK-2/3 (31), cGMP-dependent protein kinase (32), and PKC (20). We observed that erastin-induced HSPB1 phosphorylation is mediated by PKC and its attenuation by PKC inhibitor or genetic knock-down enhances erastin-induced ferroptosis. Collectively,

these findings suggest that the induction of HSPB1 phosphorylation is a universal pro-survival event against various types of cell death, including ferroptosis.

Iron is a trace element essential for fundamental metabolic processes and cell survival, but its excessive accumulation causes cell death (11, 33). For example, ferroptosis is a type of cell death resulting from an iron-dependent accumulation of lipid ROS (6), which can be prevented by iron chelation or inhibition of iron uptake, as in the use of deferoxamine (6). Although the specific role of iron in ferroptosis remains unclear, one or more iron-dependent enzymes may function as part of the oxidative lethal mechanism (6). Previously, HSPB1 was suggested as a negative regulator of intracellular iron accumulation and uptake in fibroblasts or the heart (34–36). Here, we provide evidence that overexpression of HSPB1 also inhibits erastin-induced iron uptake, whereas knockdown of HSPB1 increases erastin-induced iron uptake in cancer cells. Thus, when cancer cells contain aberrantly elevated levels of iron and HSPB1 (37, 38), the cells may be predisposed to ferroptotic cell death if the HSPB1 pathway is down-regulated.

In conclusion, our discovery of HSPB1 as a critical regulator of ferroptotic cancer cell death has provided new insights into the molecular mechanism of ferroptosis. It not only confirms the involvement of iron uptake and lipid oxidization in ferroptosis, but also provides a basis for possible combinational cancer therapy targeting both HSPB1 and ferroptosis. Given the pathogenic roles of ferroptosis in various diseases (e.g., excitotoxic cell death, Huntington's disease, periventricular leukomalacia, and renal injury) (6, 39), as well as the protective role of HSPB1 in these diseases (40), it will be important to elucidate the mechanisms underlying HSPB1-mediated ferroptosis resistance under various conditions.

Materials and Methods

Antibodies and reagents

The antibodies to HSPB1 (#H2289; 1:500), GAPDH (#G8795; 1:2000) and WAVE2 (#SAB2106929; 1:500) were obtained from Sigma (St. Louis, MO, USA). The antibodies to HSP90 (#4877; 1:1000), HSP70 (#4872; 1:1000), HSF1 (#4356; 1:1000), p-HSPB1 ser15 (#2404; 1:1000), FTH1 (#3998; 1:1000), and TFR1 (#13208; 1:1000) were obtained from Cell Signaling Technology (Danvers, MA, USA). Staurosporine (#S5921), Z-VAD-FMK (#V116), hydrogen peroxide solution (#H3410), deferoxamine (#D9533), calphostin C (#C6303), and cytochalasin D (#C8273) were obtained from Sigma (St. Louis, MO, USA). Erastin (#S7242), ferrostatin-1 (#S7243), and cyclosporin A (#S2286) were obtained from Selleck Chemicals (Houston, TX, USA). Nec-1s (#2263) was obtained from BioVision (Milpitas, CA, USA). Gö 6983 (#133053-19-7) came from EMD Millipore Corporation (Billerica, MA, USA). KRIBB3 (#CAS 129414-88-6) was obtained from Santa Cruz Biotech (Santa Cruz, CA, USA).

Cell culture

HeLa (#CCL-2), U2OS (#HTB-96), and LNCaP (#CRL-1740) cells were obtained from ATCC. These cells were grown in Dulbecco's Modified Eagle's Medium (HeLa), McCoy's

5a Modified Medium (U2OS), or RPMI-1640 Medium (LNCaP) with 10% fetal bovine serum, 2 mM L-glutamine, and 100 U/ml of penicillin and streptomycin.

Cell viability analysis

Cell viability was evaluated with an alamarBlue Cell Viability Assay Kit (#88952, Thermo Fisher Scientific Inc. Rockford, IL, USA) according the manufacturer's instructions. Described briefly, cells were plated in a 96-well plate and exposed to various concentrations of the cytotoxic compounds for an indicated time. The alamarBlue Reagent (10 μl) was added to each well, incubated at 37°C in 5% CO_2 for four hours, and then the plates were measured at 545nm/590nm (Ex/Em) using the Tecan Safire^2 Multi-detection Microplate Reader (Morrisville NC, USA). Average percentage of inhibition at each concentration was calculated as previously described.

Western blot analysis

Western blot was used to analyze protein expression as described previously (30). Described briefly, after extraction, proteins in cell lysates were first resolved by SDS-polyacrylamide gel electrophoresis and then transferred to nitrocellulose membrane and subsequently incubated with the primary antibody. After incubation with peroxidase-conjugated secondary antibodies, the signals were visualized by enhanced chemiluminescence (Pierce, Rockford, IL, USA, #32106) according to the manufacturer's instructions. The relative band intensity was quantified using the Gel-pro Analyzer® software (Media Cybernetics, Bethesda, MD, USA).

RNAi and gene transfection

The human HSF1-shRNA (SHCLNG-NM_005526_TRCN0000007480; Sequence: CCGGGCAGGTTGTTCATAGTCAGAACTCGAGTTCTGACTATGAACAACCTGCTTTTT), human HSPB1-shRNA1 (SHCLNG-NM_001540_TRCN0000342857; Sequence: CCGGGATCACCATCCCAGTCACCTTCTCGAGAAGGTGACTGGGATGGTGATCTTTTTG), human HSPB1-shRNA2 (SHCLNG-NM_001540_TRCN0000008753; Sequence:CCGGCCGATGAGACTGCCGCCAAGTCTCGAGACTTGGCGGCAGTCTCATCGGTTTTT); human WAVE2-shRNA (SHCLND-NM_006990_TRCN0000382420; Sequence: GTACCGGAGCTCTTTACTCAGGCAAATACTCGAGTATTTGCCTGAGTAAAGAGCTTTTTTTG) and control shRNA (SHC001) were obtained from Sigma (St. Louis, MO, USA). pcDNA4-HisMaxC-HSPB1 and pcDNA4-HisMaxC-S15A/S86A were kind gifts from Dr. Yoon-Jin Lee (Korea Institute of Radiological and Medical Sciences) (41). Transfections were performed with Lipofectamine™ 2000 (#11668-019, Invitrogen) as previously described (42, 43).

Heat shock treatment

Cells were sealed in screw cap flasks containing an atmosphere of 5% CO_2, 95% air. These flasks were then immersed completely in a water bath with a measured temperature of 42.5°C. By using this previously described protocol (44), the medium within the flask

reached 42.5°C within five minutes of immersion. After one hour of immersion, cells were left at 37°C for 24 hours and then treated with erastin.

Quantitative real time polymerase chain reaction

Total RNA isolation and quantitative RT-PCR or real-time RT-PCR were carried out by the procedures described previously (45). Briefly, first-strand cDNA synthesis was carried out by using a Reverse Transcription System Kit according to the manufacturer's instructions (#11801-025, OriGene Technologies, Rockville, MD, USA). cDNA from various cell samples was amplified with specific primers (HSP100/ClpB: 5'-ACACCCTTGGATTATGCCCGAG-3' and 5'-GATGTGCTCCTTTAGTCGCTGC-3'; HSP90: 5'-TCTGCCTCTGGTGATGAGATGG-3' and 5'-CGTTCCACAAAGGCTGAGTTAGC-3'; HSP70: 5'-GACCTGCCAATCGAGAATCAGC-3' and 5'-CTGCGTTCTTAGCATCATTCCGC-3'; HSP60: 5'-TGCCAATGCTCACCGTAAGCCT-3' and 5'-AGCCTTGACTGCCACAACCTGA-3'; HSP40: 5'-AGTTCAAGGAGATCGCTGAGGC-3' and 5'-GCTGAAAGAGGTACCATTGGCAC -3'; HSPB1:5'-CTGACGGTCAAGACCAAGGATG-3' and 5'-GTGTATTTCCGCGTGAAGCACC-3'; HSF1:5'-TGAAAAGTGCCTCAGCGTAGCC-3' and 5'-TGCTCAGCATGGTCTGCAGGTT-3'; PTGS2:5'-CGGTGAAACTCTGGCTAGACAG-3' and 5'-GCAAACCGTAGATGCTCAGGGA-3') and the data was normalized to 18S ribosomal RNA (5'-CTTAGAGGGACAAGTGGCG-3' and 5'-ACGCTGAGCCAGTCAGTGTA-3').

Iron assay

The relative iron concentration in cell lysates was assessed using an Iron Assay Kit (#ab83366, Abcam) according the manufacturer's instructions. This kit provides a simple convenient means of measuring ferrous and/or ferric iron in samples. In the assay, ferric carrier protein dissociates ferric iron into a solution in the presence of acid buffer. After reduction to the ferrous form (Fe^{2+}), iron reacts with Ferene S to produce a stable colored complex and give absorbance at 593 nm.

Lipid ROS assay

Fluorometric analysis of lipid ROS production was carried out using dye C11-BODIPY (#D-3861, Life Technologies, USA) as previously described (6). Oxidation of the polyunsaturated butadienyl portion of the dye resulted in a shift of the fluorescence emission peak from ~590 nm to ~510 nm.

Caspase 3 activity assay

Caspase 3 activity was assessed using a Caspase 3 Assay Kit (#ab39700, Abcam) according the manufacturer's instructions.

LDH release assay

LDH release was assessed using a LDH Assay Kit (#ab65393, Abcam) according the manufacturer's instructions.

p-HSF1 (Ser326) assay

The relative determination of HSF1 phosphorylated at Ser326 in cell lysates was assessed using a HSF1 (pSer326) ELISA Kit (#ab136939, Abcam) according the manufacturer's instructions.

Xenograftment assay in NOD/SCID mice

Indicated HeLa cells were subcutaneously injected into the dorsal flanks right of the midline in SCID mice (weight ~20g). At day seven, mice were injected with erastin (20 mg/kg/ i.v., twice daily every other day) with or without KRIBB3 (50 mg/kg/ i.p., once daily every other day) for two weeks. The erastin ($C_{30}H_{31}ClN_4O_4$) was bought from Selleck Chemicals. Erastin was dissolved in vehicle (2% DMSO and 98% phosphate buffered saline) and prepared by Ultrasonic Cleaner (Fisher Scientific). A final volume of 300 ul erastin was applied through the tail vein. The half-life and area under curve (0-t) of erastin are 27 min and 173 μg.min/ml, respectively. The Rodent Tail Vein Catheter (Braintree Scientific, MTV#1) were used to perform injection. This system allows easier access for both timed injections and repeated bolus administration. Tumors were measured once a week. The volumes were calculated using the following formula: volume (mm^3)=length×width^2×π/6. This study was approved by the Third Affiliated Hospital of Guangzhou Medical University and the University of Pittsburgh Institutional Animal Care and Use Committees and performed in accordance with the Association for Assessment and Accreditation of Laboratory Animal Care guidelines (http://www.aaalac.org).

Statistical analysis

Unless otherwise indicated, data are expressed as means ± SD and were evaluated using an ANOVA LSD test. P values < 0.05 were considered statistically significant.

Acknowledgements

We thank Christine Heiner (Department of Surgery, University of Pittsburgh) for her critical reading of the manuscript. This work was supported by the National Institutes of Health (R01CA160417 to D.T.), a 2013 Pancreatic Cancer Action Network-AACR Career Development Award (Grant Number 13-20-25-TANG), The National Natural Science Foundation-Guangdong Joint Fund (U1132005 to X.S.), and Science and Information Technology of Guangzhou Key Project (2011Y1-00038 to X.S.). H.W. is supported by grants from the National Center of Complementary and Alternative Medicine (R01AT005076) and the National Institute of General Medical Sciences (R01GM063075).

References

1. Galluzzi L, Vitale I, Abrams JM, Alnemri ES, Baehrecke EH, Blagosklonny MV, et al. Molecular definitions of cell death subroutines: recommendations of the Nomenclature Committee on Cell Death 2012. Cell Death Differ. 2012 Jan; 19(1):107–120. [PubMed: 21760595]
2. Galluzzi L, Bravo-San Pedro JM, Vitale I, Aaronson SA, Abrams JM, Adam D, et al. Essential versus accessory aspects of cell death: recommendations of the NCCD 2015. Cell Death Differ. 2014 Sep 19.
3. Fuchs Y, Steller H. Programmed cell death in animal development and disease. Cell. 2011 Nov 11; 147(4):742–758. [PubMed: 22078876]
4. Vanden Berghe T, Linkermann A, Jouan-Lanhouet S, Walczak H, Vandenabeele P. Regulated necrosis: the expanding network of non-apoptotic cell death pathways. Nat Rev Mol Cell Biol. 2014 Feb; 15(2):135–147. [PubMed: 24452471]

5. Tait SW, Ichim G, Green DR. Die another way--non-apoptotic mechanisms of cell death. J Cell Sci. 2014 May 15; 127(Pt 10):2135–2144. [PubMed: 24833670]
6. Dixon SJ, Lemberg KM, Lamprecht MR, Skouta R, Zaitsev EM, Gleason CE, et al. Ferroptosis: an iron-dependent form of nonapoptotic cell death. Cell. 2012 May 25; 149(5):1060–1072. [PubMed: 22632970]
7. Dixon SJ, Patel DN, Welsch M, Skouta R, Lee ED, Hayano M, et al. Pharmacological inhibition of cystine-glutamate exchange induces endoplasmic reticulum stress and ferroptosis. Elife (Cambridge). 2014; 3:e02523.
8. Dolma S, Lessnick SL, Hahn WC, Stockwell BR. Identification of genotype-selective antitumor agents using synthetic lethal chemical screening in engineered human tumor cells. Cancer Cell. 2003 Mar; 3(3):285–296. [PubMed: 12676586]
9. Yagoda N, von Rechenberg M, Zaganjor E, Bauer AJ, Yang WS, Fridman DJ, et al. RAS-RAF-MEK-dependent oxidative cell death involving voltage-dependent anion channels. Nature. 2007 Jun 14; 447(7146):864–868. [PubMed: 17568748]
10. Yang WS, Stockwell BR. Synthetic lethal screening identifies compounds activating iron-dependent, nonapoptotic cell death in oncogenic-RAS-harboring cancer cells. Chem Biol. 2008 Mar; 15(3):234–245. [PubMed: 18355723]
11. Dixon SJ, Stockwell BR. The role of iron and reactive oxygen species in cell death. Nat Chem Biol. 2014 Jan; 10(1):9–17. [PubMed: 24346035]
12. Yang WS, SriRamaratnam R, Welsch ME, Shimada K, Skouta R, Viswanathan VS, et al. Regulation of ferroptotic cancer cell death by GPX4. Cell. 2014 Jan 16; 156(1–2):317–331. [PubMed: 24439385]
13. Friedmann Angeli JP, Schneider M, Proneth B, Tyurina YY, Tyurin VA, Hammond VJ, et al. Inactivation of the ferroptosis regulator Gpx4 triggers acute renal failure in mice. Nat Cell Biol. 2014 Dec; 16(12):1180–1191. [PubMed: 25402683]
14. Linkermann A, Skouta R, Himmerkus N, Mulay SR, Dewitz C, De Zen F, et al. Synchronized renal tubular cell death involves ferroptosis. Proc Natl Acad Sci U S A. 2014 Nov 25; 111(47): 16836–16841. [PubMed: 25385600]
15. Georgopoulos C, Welch WJ. Role of the major heat shock proteins as molecular chaperones. Annu Rev Cell Biol. 1993; 9:601–634. [PubMed: 8280473]
16. Wu C. Heat shock transcription factors: structure and regulation. Annu Rev Cell Dev Biol. 1995; 11:441–469. [PubMed: 8689565]
17. Takayama S, Reed JC, Homma S. Heat-shock proteins as regulators of apoptosis. Oncogene. 2003 Dec 8; 22(56):9041–9047. [PubMed: 14663482]
18. Ramanathan R, Mancini RA, Suman SP, Beach CM. Covalent binding of 4-hydroxy-2-nonenal to lactate dehydrogenase decreases NADH formation and metmyoglobin reducing activity. J Agric Food Chem. 2014 Mar 5; 62(9):2112–2117. [PubMed: 24552270]
19. Guettouche T, Boellmann F, Lane WS, Voellmy R. Analysis of phosphorylation of human heat shock factor 1 in cells experiencing a stress. BMC Biochem. 2005; 6:4. [PubMed: 15760475]
20. Xu L, Chen S, Bergan RC. MAPKAPK2 and HSP27 are downstream effectors of p38 MAP kinase-mediated matrix metalloproteinase type 2 activation and cell invasion in human prostate cancer. Oncogene. 2006 May 18; 25(21):2987–2998. [PubMed: 16407830]
21. Lavoie JN, Hickey E, Weber LA, Landry J. Modulation of actin microfilament dynamics and fluid phase pinocytosis by phosphorylation of heat shock protein 27. J Biol Chem. 1993 Nov 15; 268(32):24210–24214. [PubMed: 8226968]
22. Rousseau S, Houle F, Landry J, Huot J. p38 MAP kinase activation by vascular endothelial growth factor mediates actin reorganization and cell migration in human endothelial cells. Oncogene. 1997 Oct; 15(18):2169–2177. [PubMed: 9393975]
23. Takenawa T, Suetsugu S. The WASP-WAVE protein network: connecting the membrane to the cytoskeleton. Nat Rev Mol Cell Biol. 2007 Jan; 8(1):37–48. [PubMed: 17183359]
24. Shin KD, Lee MY, Shin DS, Lee S, Son KH, Koh S, et al. Blocking tumor cell migration and invasion with biphenyl isoxazole derivative KRIBB3, a synthetic molecule that inhibits Hsp27 phosphorylation. J Biol Chem. 2005 Dec 16; 280(50):41439–41448. [PubMed: 16234246]

25. Fulda S, Gorman AM, Hori O, Samali A. Cellular stress responses: cell survival and cell death. Int J Cell Biol. 2010; 2010:214074. [PubMed: 20182529]
26. Zhang Q, Kang R, Zeh HJ 3rd, Lotze MT, Tang D. DAMPs and autophagy: cellular adaptation to injury and unscheduled cell death. Autophagy. 2013 Apr; 9(4):451–458. [PubMed: 23388380]
27. Carver JA, Rekas A, Thorn DC, Wilson MR. Small heat-shock proteins and clusterin: intra- and extracellular molecular chaperones with a common mechanism of action and function? IUBMB Life. 2003 Dec; 55(12):661–668. [PubMed: 14769002]
28. Jakob U, Gaestel M, Engel K, Buchner J. Small heat shock proteins are molecular chaperones. J Biol Chem. 1993 Jan 25; 268(3):1517–1520. [PubMed: 8093612]
29. Huot J, Houle F, Spitz DR, Landry J. HSP27 phosphorylation-mediated resistance against actin fragmentation and cell death induced by oxidative stress. Cancer Res. 1996 Jan 15; 56(2):273–279. [PubMed: 8542580]
30. Tang D, Kang R, Livesey KM, Kroemer G, Billiar TR, Van Houten B, et al. High-mobility group box 1 is essential for mitochondrial quality control. Cell Metab. 2011 Jun 8; 13(6):701–711. [PubMed: 21641551]
31. Guay J, Lambert H, Gingras-Breton G, Lavoie JN, Huot J, Landry J. Regulation of actin filament dynamics by p38 map kinase-mediated phosphorylation of heat shock protein 27. J Cell Sci. 1997 Feb; 110(Pt 3):357–368. [PubMed: 9057088]
32. Butt E, Immler D, Meyer HE, Kotlyarov A, Laass K, Gaestel M. Heat shock protein 27 is a substrate of cGMP-dependent protein kinase in intact human platelets: phosphorylation-induced actin polymerization caused by HSP27 mutants. J Biol Chem. 2001 Mar 9; 276(10):7108–7113. [PubMed: 11383510]
33. Hentze MW, Muckenthaler MU, Galy B, Camaschella C. Two to tango: regulation of Mammalian iron metabolism. Cell. 2010 Jul 9; 142(1):24–38. [PubMed: 20603012]
34. Chen H, Zheng C, Zhang Y, Chang YZ, Qian ZM, Shen X. Heat shock protein 27 downregulates the transferrin receptor 1-mediated iron uptake. Int J Biochem Cell Biol. 2006; 38(8):1402–1416. [PubMed: 16546437]
35. Arrigo AP, Virot S, Chaufour S, Firdaus W, Kretz-Remy C, Diaz-Latoud C. Hsp27 consolidates intracellular redox homeostasis by upholding glutathione in its reduced form and by decreasing iron intracellular levels. Antioxid Redox Signal. 2005 Mar-Apr;7(3–4):414–422. [PubMed: 15706088]
36. Zhang X, Min X, Li C, Benjamin IJ, Qian B, Ding Z, et al. Involvement of reductive stress in the cardiomyopathy in transgenic mice with cardiac-specific overexpression of heat shock protein 27. Hypertension. 2010 Jun; 55(6):1412–1417. [PubMed: 20439823]
37. Torti SV, Torti FM. Iron and cancer: more ore to be mined. Nat Rev Cancer. 2013 May; 13(5): 342–355. [PubMed: 23594855]
38. Oesterreich S, Weng CN, Qiu M, Hilsenbeck SG, Osborne CK, Fuqua SA. The small heat shock protein hsp27 is correlated with growth and drug resistance in human breast cancer cell lines. Cancer Res. 1993 Oct 1; 53(19):4443–4448. [PubMed: 8402609]
39. Skouta R, Dixon SJ, Wang J, Dunn DE, Orman M, Shimada K, et al. Ferrostatins inhibit oxidative lipid damage and cell death in diverse disease models. J Am Chem Soc. 2014 Mar 26; 136(12): 4551–4556. [PubMed: 24592866]
40. Vidyasagar A, Wilson NA, Djamali A. Heat shock protein 27 (HSP27): biomarker of disease and therapeutic target. Fibrogenesis Tissue Repair. 2012; 5(1):7. [PubMed: 22564335]
41. Lee YJ, Lee DH, Cho CK, Bae S, Jhon GJ, Lee SJ, et al. HSP25 inhibits protein kinase C delta-mediated cell death through direct interaction. J Biol Chem. 2005 May 6; 280(18):18108–18119. [PubMed: 15731106]
42. Huang J, Ni J, Liu K, Yu Y, Xie M, Kang R, et al. HMGB1 promotes drug resistance in osteosarcoma. Cancer Res. 2012 Jan 1; 72(1):230–238. [PubMed: 22102692]
43. Livesey KM, Kang R, Vernon P, Buchser W, Loughran P, Watkins SC, et al. p53/HMGB1 complexes regulate autophagy and apoptosis. Cancer Res. 2012 Apr 15; 72(8):1996–2005. [PubMed: 22345153]

44. Tang D, Shi Y, Jang L, Wang K, Xiao W, Xiao X. Heat shock response inhibits release of high mobility group box 1 protein induced by endotoxin in murine macrophages. Shock. 2005 May; 23(5):434–440. [PubMed: 15834309]

45. Yang L, Xie M, Yang M, Yu Y, Zhu S, Hou W, et al. PKM2 regulates the Warburg effect and promotes HMGB1 release in sepsis. Nature communications. 2014; 5:4436.

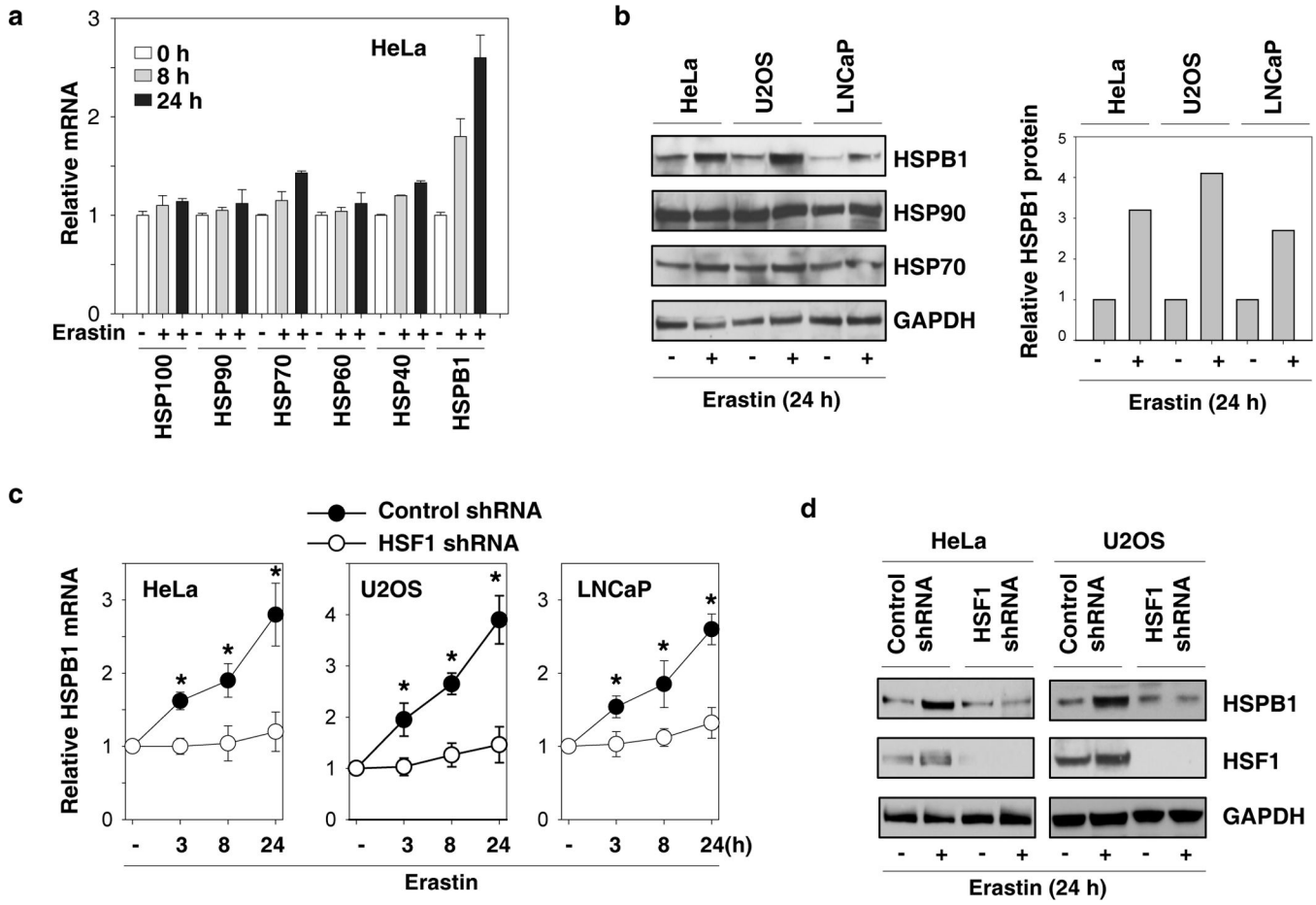

Figure 1. Erastin induces HSF1-dependent HSPB1 expression in human cancer cells

(A) HeLa cells were treated with erastin (0.5 μM) for eight hours and 24 hours, and mRNA expressions of indicated HSPs were assayed by Q-PCR (n=3). (B) Indicated human cancer cells were treated with erastin (HeLa, 0.5 μM; U2OS, 5 μM; LNCaP, 5 μM) for 24 hours and the protein expressions of indicated HSPs were assayed by Western blot. (C, D) Indicated human cancer cells were transfected with control shRNA and HSF1 shRNA for 48 hours and treated with erastin (HeLa, 0.5 μM; U2OS, 5 μM; LNCaP, 5 μM) for 3–24 h. The mRNA expressions of HSPB1 (C) were assayed by Q-PCR (n=3, *$p < 0.05$ versus control shRNA group). In parallel, the protein expressions of HSPB1 and HSF1 (D) were assayed using Western blot.

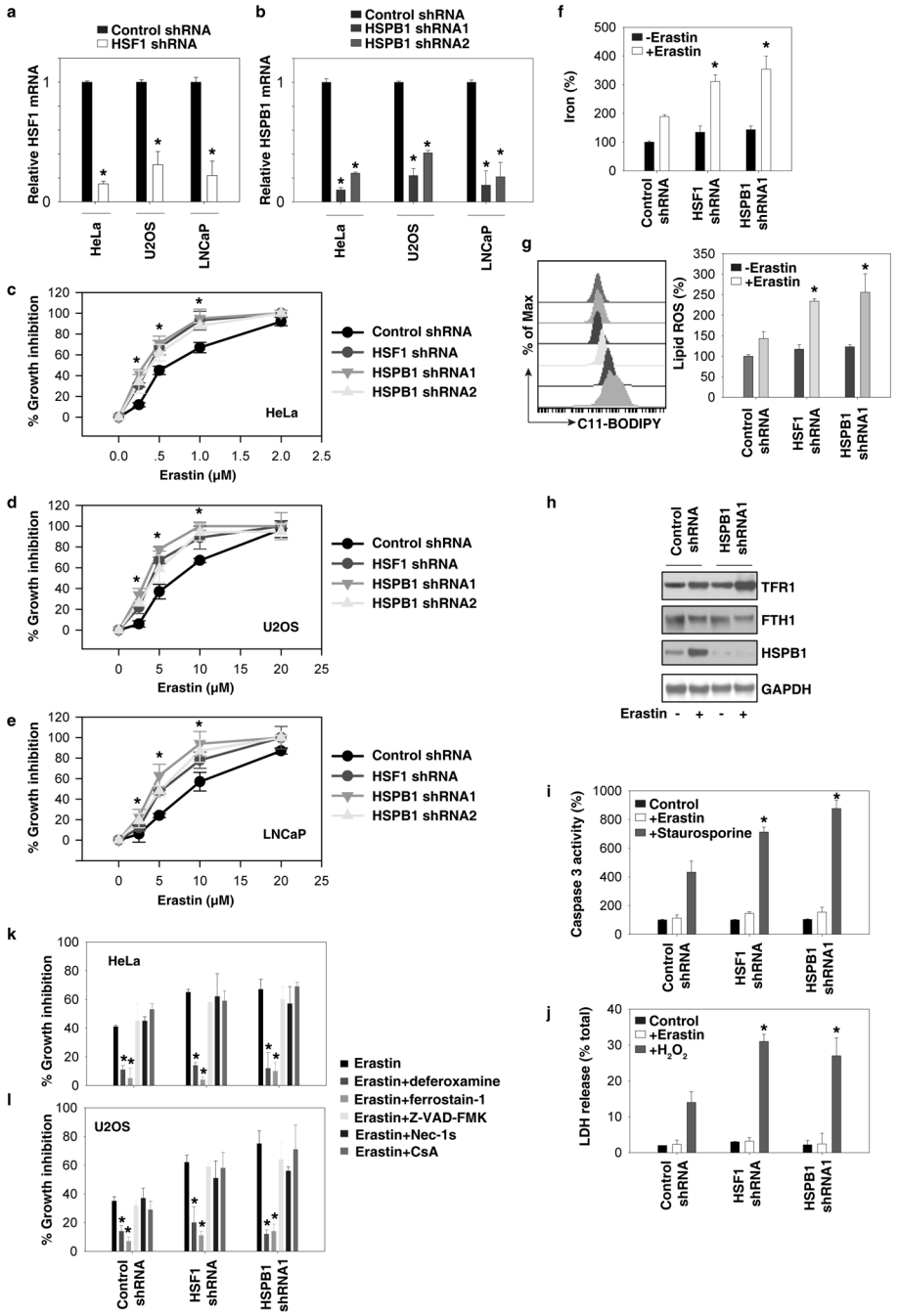

Figure 2. Inhibition of HSF1-dependent HSPB1 expression increased erastin-induced ferroptosis

(A, B) Q-PCR analysis of HSF1 (A) and HSPB1 (B) mRNA expression in indicated knockdown cells (n=3, *p <0.05 versus control shRNA group). (C–E) Effects of knockdown of HSF1 and HSPB1 on erastin-induced growth inhibition at 24 hours in HeLa (C), U2OS (D), and LNCaP (E) cells. (F–I), Analysis of intracellular iron (F), lipid ROS (G), TFR1 (H), FTH1 (H), caspase 3 activity (I), and LDH release (J) in indicated HeLa cells after treatment with erastin (0.5 μM, 24h), staurosporine (1 μM, 24h), or H_2O_2 (10 mM, 2h) (n=3, *p < 0.05 versus control shRNA group). (K, L) Effects of deferoxamine (100 μM), ferrostain-1 (1

μM), Z-VAD-FMK (10 μM), necrostain 1s (Nec-1s, 10 μM), and cyclosporin A (CsA, 5 μM) on erastin-induced growth inhibition at 24 hours in indicated HeLa (J) and U2OS (K) cells (n=3, *p < 0.05 versus erastin group).

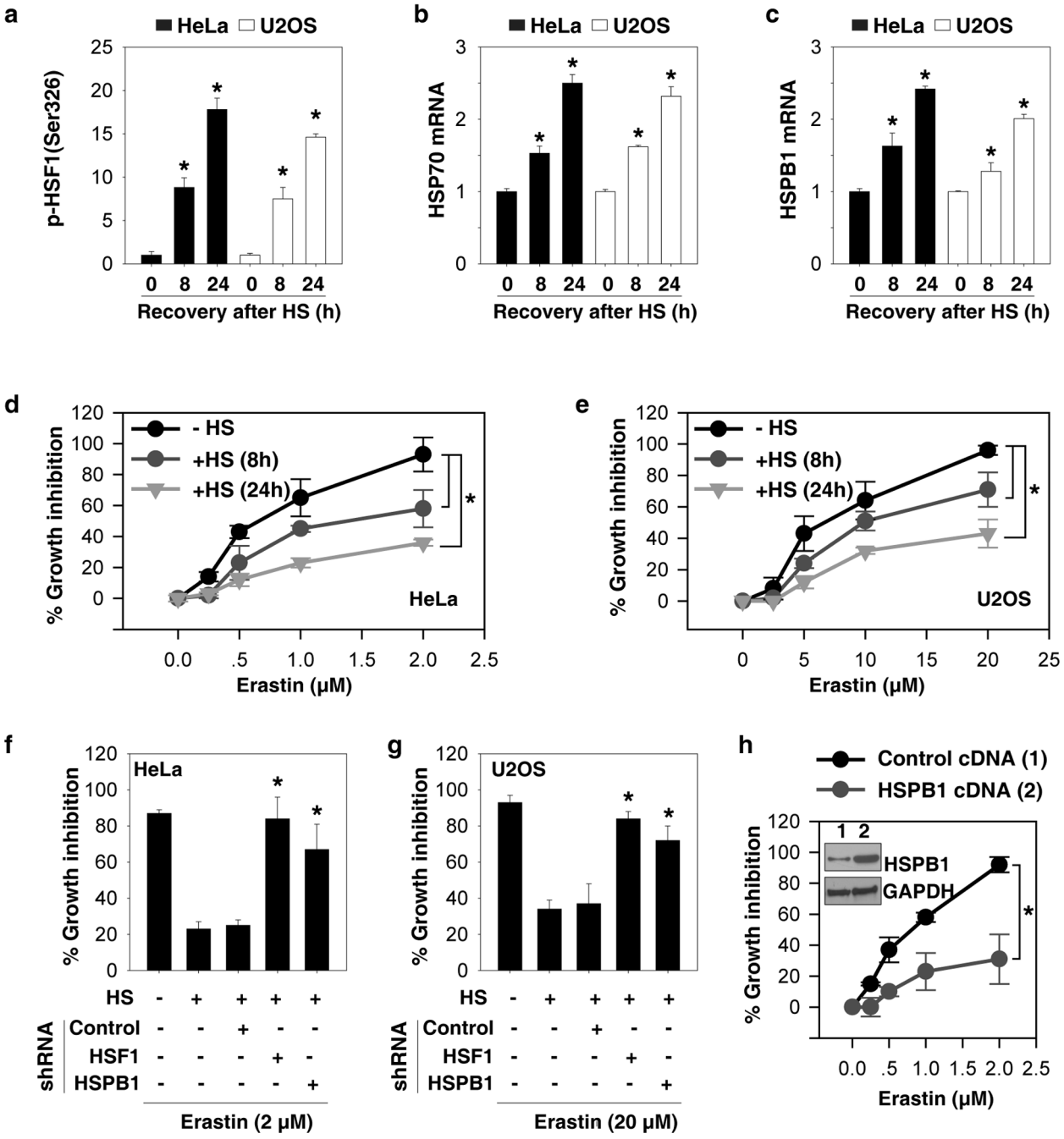

Figure 3. HSPB1 overexpression inhibits erastin-induced ferroptosis

(A–C) Indicated cells were heated at 42.5°C for one hour and then returned to 37°C, and samples were obtained at eight and 24 h after heat shock ("HS"). The p-HSF1 (Ser326) (A), HSP70 mRNA (B), and HSPB1 mRNA (C) were assayed (n=3, *p < 0.05 versus control group). (D, E) Effects of heat shock pretreatment on erastin-induced growth inhibition at 24 hours in indicated HeLa (D) and U2OS (E) cells (n=3, *p < 0.05). (F, G) Effects of knockdown of HSF1 and HSPB1 on heat shock pretreatment-mediated protection against erastin-induced growth inhibition at 24 hours in indicated HeLa (F) and U2OS (G) cells

(n=3, *p < 0.05 versus control shRNA group). (H) Effects of HSPB1 overexpression ("HSPB1 cDNA") by gene transfection on erastin-induced growth inhibition at 24 hours in HeLa cells (n=3, *p < 0.05).

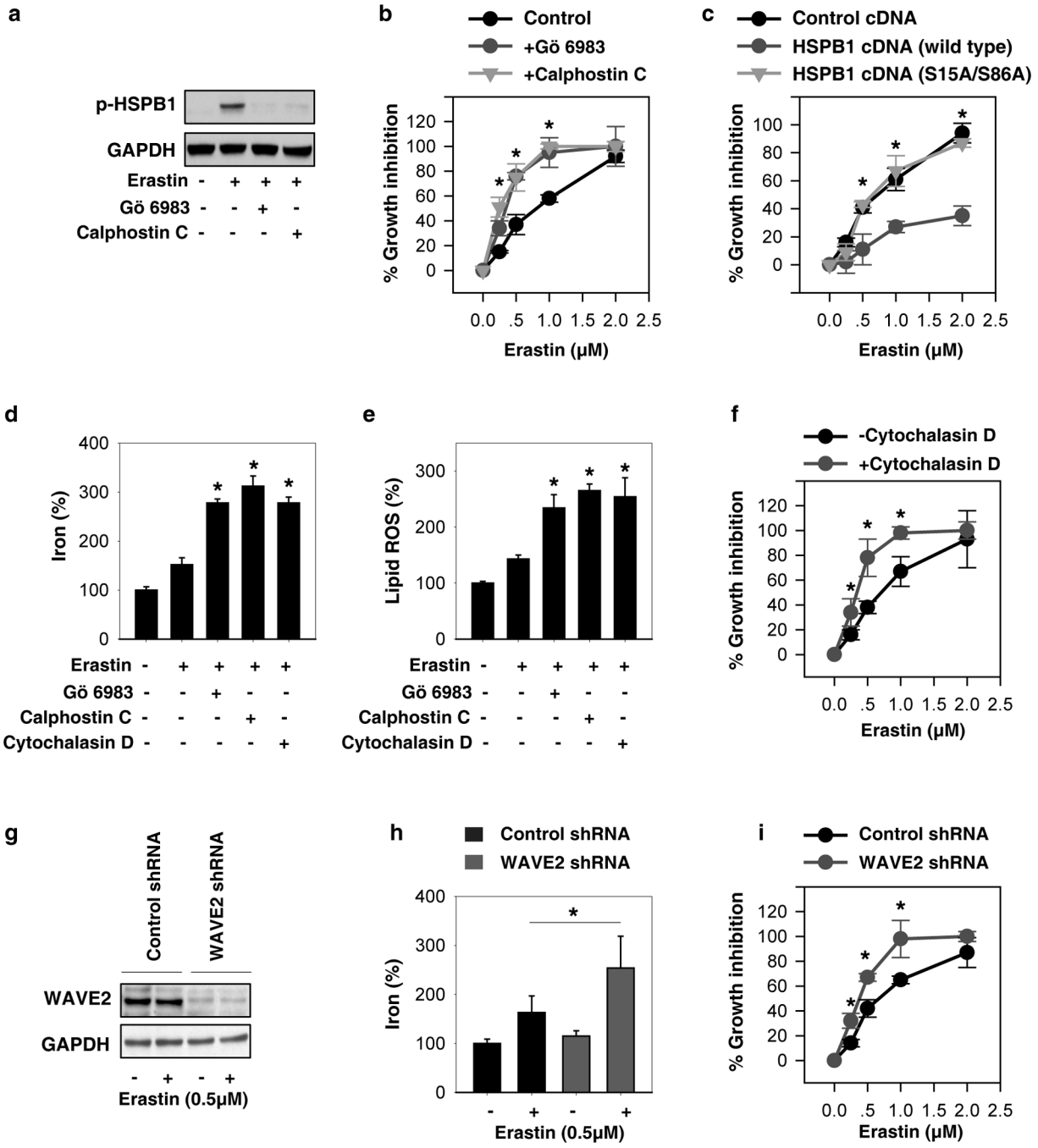

Figure 4. HSPB1 phosphorylation-mediated resistance to erastin-induced ferroptosis

(A) HeLa cells were treated with erastin (0.5 μM) for 24 hours with or without Go 6893 (0.5 μM) and calphostin C (0.1 μM), and HSPB1 phosphorylation at Ser 15 was assayed using Western blot. (B) Effects of Go 6893 and calphostin C on erastin-induced growth inhibition at 24 hours in HeLa cells (n=3, *p < 0.05 versus control group). (C) Effects of phosphorylation-deficient mutants of HSPB1 (S15A/S86A) on erastin-induced growth inhibition at 24 hours in HeLa cells (n=3, *p < 0.05 versus HSPB1 cDNA group). (D, E) Analysis of intracellular iron (D) and lipid ROS (E) in HeLa cells after treatment with

erastin (0.5 μM), Go 6893 (0.5 μM), calphostin C (0.1 μM), and cytochalasin D (0.5 μM) for 24 h (n=3, *p < 0.05 versus control erastin group). (F) Effects of cytochalasin D (0.5 μM) on erastin-induced growth inhibition at 24 hours in HeLa cells (n=3, *p < 0.05 versus control group).(G–I) Effects of knockdown of WAVE2 (G) on erastin-induced intracellular iron (H) and growth inhibition (I) at 24 hours in HeLa cells (n=3, *p < 0.05 versus control shRNA group).

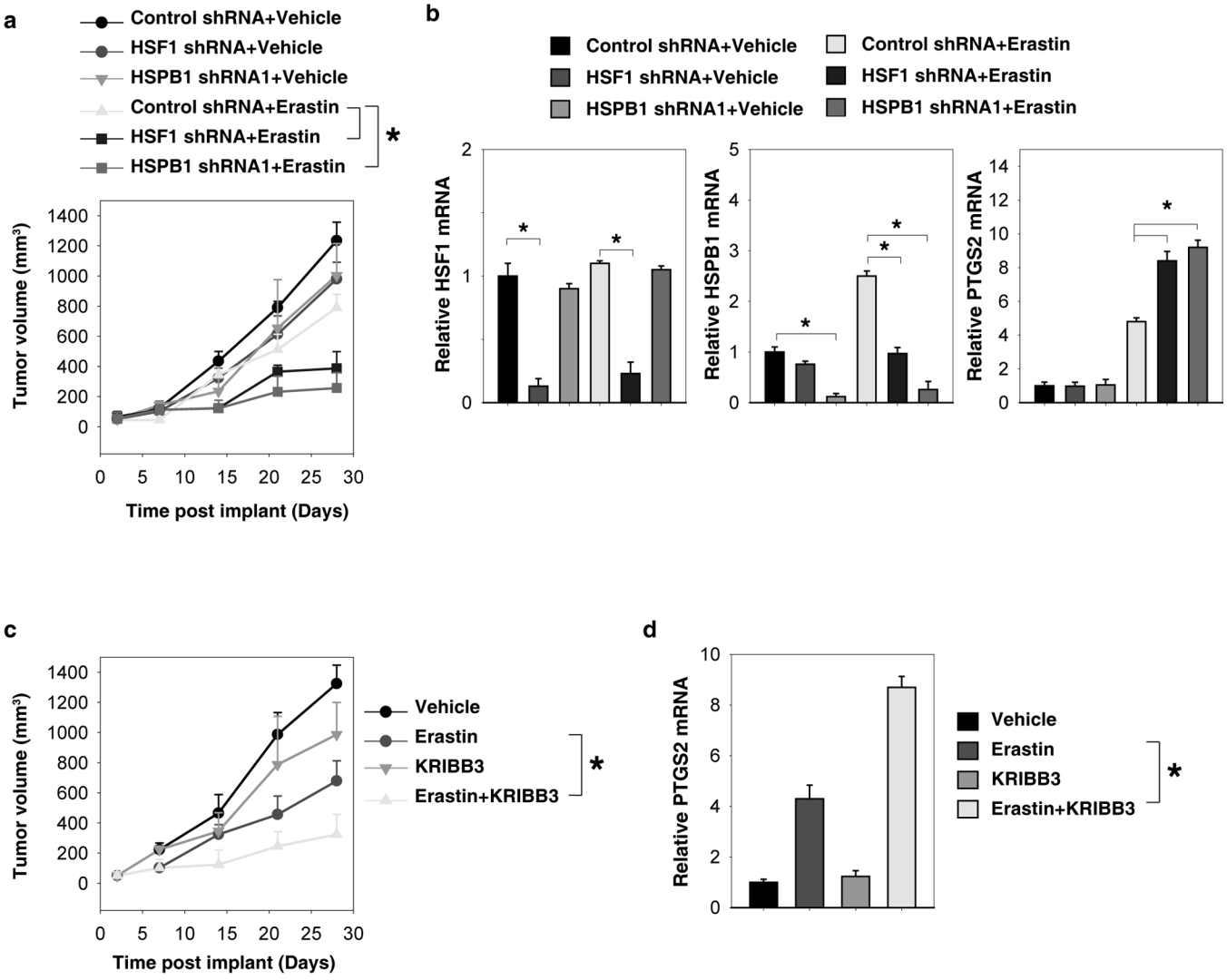

Figure 5. Suppression of the HSF1-HSPB1 pathway increases anticancer activity of erastin *in vivo*

(A) HSF1 and HSPB1 knockdown HeLa cells were more sensitive to erastin *in vivo*. SCID mice were injected subcutaneously with indicated HeLa cells (1×10^6 cells/mouse) and treated with erastin (20 mg/kg/ i.v., twice every other day) at day seven for two weeks. Tumor volume was calculated weekly. Data represents mean ± SE (n=5–8 mice/group, * $p < 0.05$). (B) Q-PCR analysis of the indicated gene expression in isolated tumor at day 28. (C) KRIBB3 increased anticancer activity of erastin *in vivo*. SCID mice were injected subcutaneously with indicated HeLa cells (1×10^6 cells/mouse) and treated with erastin (20 mg/kg/ i.v., twice every other day) with or without KRIBB3 (50 mg/kg/ i.p., once every other day) at day seven for two weeks. Tumor volume was calculated weekly. Data represent mean ± SE (n=5 mice/group, * $p < 0.05$). (B) Q-PCR analysis of the PTGS2 gene expression in isolated tumor at day 28.